

Emission Radiation from MARFES in JET

M G O'Mullane^{1,2}, R Giannella, K D Lawson¹,
N J Peacock¹, H P Summers.

JET Joint Undertaking, Abingdon, Oxon, OX14 3EA.

¹ Culham Laboratory, UKAEA/Euratom Fusion Association,
Abingdon, Oxon, OX14 3DB.

² Physics Department, University College Cork, Ireland.

"This document is intended for publication in the open literature. It is made available on the understanding that it may not be further circulated and extracts may not be published prior to publication of the original, without the consent of the Publications Officer, JET Joint Undertaking, Abingdon, Oxon, OX14 3EA, UK".

"Enquiries about Copyright and reproduction should be addressed to the Publications Officer, JET Joint Undertaking, Abingdon, Oxon, OX14 3EA".

EMISSION RADIATION FROM MARFES IN JET

M G O'Mullane^{1,2}, R Giannella, K D Lawson¹, N J Peacock¹, H P Summers

JET Joint Undertaking, Abingdon, Oxon, OX14 3EA

¹ Culham Laboratory, UKAEA/Euratom Fusion Association, Abingdon, Oxon, OX14 3DB

² Physics Department, University College Cork, Ireland

Introduction

The edge plasma has an influential part to play in determining the confinement and stability of tokamak plasma. The marfe [1] is a region of relatively cold ($T_e^m < 70\text{eV}$) and dense edge plasma which radiates strongly and can account for a significant fraction of the total radiation. In JET, as in other tokamaks, marfes are toroidally symmetric but exhibit marked poloidal asymmetry on the high field side of the tokamak. *eg.* In #20307 the poloidal location is $135^\circ \leq \theta \leq 170^\circ$ as seen in fig.1. The radial extent of the marfe is $\Delta r_m/2 \simeq 25\text{cm}$. This paper addresses the content of intrinsic plasma impurities in this isolated region.

Phenomenology

Two marfe events are reported here (#20017 and #20307). The vacuum vessel had carbon limiters with beryllium evaporation which lowers the oxygen impurity concentration from to $\sim 0.1\%$ of n_e [2]. Thus it is unlikely that there is any substantial contribution from oxygen to the marfe radiation. Both shots were limiter discharges. Although the duration of the marfes is different (5.1s and 2.1s) both discharges terminate in a density limit disruption when radiation — primarily from the marfe — exceeds the input power.

The formation phase of the marfe is preceded by a build-up of radiation at both limiters. Then the D_α , CIII, BeII and HeI radiation from the upper belt limiter fall sharply within 150ms and do not recover for the remainder of the discharge (fig.2) which suggests an inward movement of the plasma away from the limiters. Following this event a sharp spike of 20ms duration is seen in all bolometer and poloidal bremsstrahlung channels. At the end of the formation phase the bolometers show a region of enhanced radiation at the upper inner wall. For #20017 the radiated power flux, in the channel directly viewing the marfe, increases by a factor of 20 over the pre-marfe level. The marfe remains in this stationary position for $\sim 0.9\text{s}$. The position and size of the marfe is best unfolded from the 2-D bolometer data. For both discharges the marfe volume is estimated at 7.4m^3 with a elliptical cross-section of radii 0.12m and length of 0.6m. The total excess radiated power density (P_m) is $2.83 \times 10^5 \text{Wm}^{-3}$. The MHD data indicate no change in the poloidal or toroidal magnetic fields during the formation and stationary phase of the marfe.

The subsequent evolution of the marfe's position in time is illustrated in fig.3 which shows the radiation profile along the inner wall of JET. The bulk of the marfe remains

in the upper half of the tokamak but there is periodic smearing along the entire inner wall. The frequency of these excursions, from the bremsstrahlung monitors, increases from 20Hz to 50Hz as the marfe attains a final elongated structure.

The spectral observations of the marfe come from the VUV survey spectrometer on JET. The line of sight is inclined at an angle of $\sim 6^\circ$ below the midplane so the marfe is not observed directly except when the marfe structure passes through the midplane. There are two distinct aspects to the observed radiation; firstly an increase of line brightness of carbon and chlorine (CII and CIVI) which is characteristic of enhanced edge radiation and secondly a broad spectral feature between 110Å and 160Å (fig.4) which arises during the oscillation of the marfe material along the inner wall. There is a steady rise in intensity during this period. The short wavelength feature accounts for up to 30% of the total radiated power for #20017. Calculations of the wavelengths and intensities with the *ab initio* Cowan code [3] for nickel ions, NiVII to NiIX with configurations $3p^63d^m-3p^53d^{m+1}$, $(3p^63d^{m-1})4p,4f,5p,5f$ with $m = 3-1$ are shown in fig.4 convolved with the SPRED instrument function. There is a correlation between this feature of the disturbed plasma and these lowly ionised stages of nickel.

Before the marfe formation $n_e = 1.9 \times 10^{19} \text{m}^{-3}$ with $T_e = 400 \text{eV}$. Typical values of T_e in the marfe are of the order of $\sim 5-30 \text{eV}$ [1] which is consistent with the enhanced radiation from lowly ionised carbon. From pressure balance the corresponding marfe electron density is $\sim 2.6 \times 10^{20} \text{m}^{-3}$.

Radiation Modelling

Ions giving rise to marfe radiation can come from two sources: neutral and lowly ionised ions enter the plasma or ions already in the plasma stream through the marfe.

The power density radiated by an impurity of density n_z as a function of time is

$$P_{tot}(t) = n_e n_z \sum_z \frac{n_z(t)}{n_z} (P_{zL}(T_e) + P_{zR}(T_e, n_e) + P_{zB}(T_e))$$

$$\frac{dn_z}{dt} = n_e [-n_z S_z + n_{z-1} S_{z-1} - n_z \alpha_z + n_{z+1} S_{z+1}]$$

where L,R,B represent line, recombination and bremsstrahlung radiation. All atomic data is taken from the ADAS [3] system. Charge exchange is included in the calculation and is significant for neutral deuterium densities exceeding 10^{15}m^{-3} at marfe temperatures, altering the ionisation balance within the marfe.

For an ion influx entering the plasma there are only neutral and singly ionised stages which have sputtering energies of few eV. The radial balance of populations for ions already in the plasma is given by a diffusive-convective transport model SANC0[5].

The transient energy, $E^m = \int_0^m P^m dt$, is the energy radiated during the ions movement through the marfe. The results for carbon and nickel are given in fig.5 and fig.6

for the two different initial conditions. Ions entering the plasma quickly reach an equilibrium (within 0.07ms at 30eV for carbon), although at lower temperatures this process takes longer (2.4ms at 10eV) whereas, when ions stream through the marfe the slower recombination rates mean that a much longer time (~ 25 ms) is required. The radiation emitted by neutrals ionising towards equilibrium can exceed by up to a factor of 100 that at equilibrium.

The power radiated depends on the transit time of the impurities in the marfe. With $q_{\text{eff}} \simeq 4.4$ the ion travels ~ 12 m through the marfe. The impurity ion suffers many collisions in the marfe and is slowed down within a few microseconds. For ions, at the marfe thermal velocity, the transit times are $t_C^m = 0.54$ ms and $t_{Ni}^m = 1.2$ ms. The cross-field diffusion times are up to a factor of 100 times slower than the streaming through time. The ionisation rates are such that re-ionisation is quick and the poloidal asymmetry is maintained by the rapid rethermalisation of electrons exiting the marfe.

The distribution of the marfe radiated power is estimated to be 70% carbon and 30% nickel. In these discharges Z_{eff} is measured to be ~ 1.7 which gives a carbon concentration $0.025n_e$. In these discharges the typical nickel concentration is expected to be $10^{-4}n_e$ to $10^{-5}n_e$. The observed radiated power density is related to the transient energy by

$$P^m = \frac{E^m AN_i v_i}{V^m}$$

where i refers to the impurity. The observed radiation can be explained with a carbon concentration of $5.7 \times 10^{-3}n_e$ with $8.0 \times 10^{-4}n_e$ of nickel. There is no need to appeal to an influx of neutral particles which is consistent with the unchanging Z_{eff} .

If an influx is to be used to explain the observed radiation the number of particles/second required for carbon is $\sim 3 \times 10^{21}$ at 20eV with 1.5×10^{19} particles/second for nickel. This would appear to be unexpectedly high for nickel given that there are no known sources neighbouring the marfe. This suggests that nickel streaming through the marfe is the radiating mechanism.

[1] Lipschultz B *et al* Nucl. Fusion. 24 p977 1984

[2] Lawson KD *et al* Proc. 17th EPS Amsterdam, 1990 part 3, p1413

[3] Cowan RD *Theory of Atomic Structure and Spectra* University of California Press 1981

[4] Summers HP and von Hellermann M in *Atomic and Plasma-Material Interaction Processes in Controlled Thermonuclear Fusion* Editor JK Janev, Elsevier, Amsterdam (1993)

[5] Lauro-Taroni L, In preparation (1993)

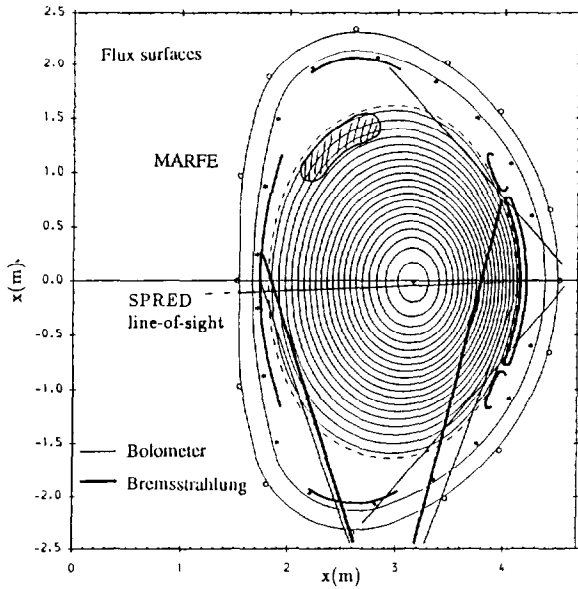


fig.1 Position of marfe for shot 20307 with approximate location of bolometer and bremsstrahlung poloidal arrays

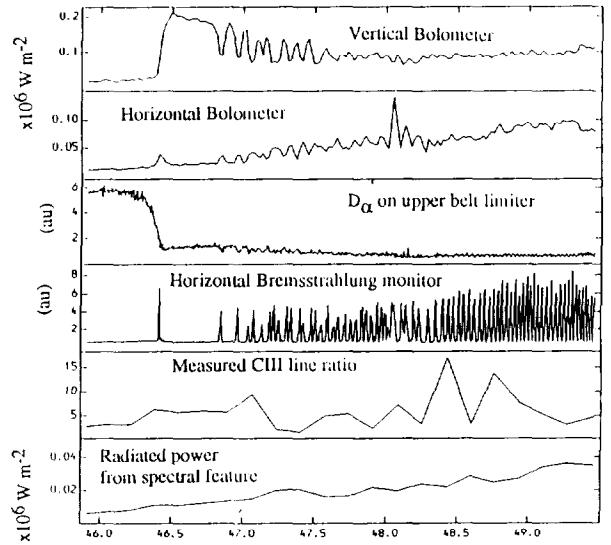


fig.2 Evolution of the marfe for shot 20017 The marfe forms at 46.4s

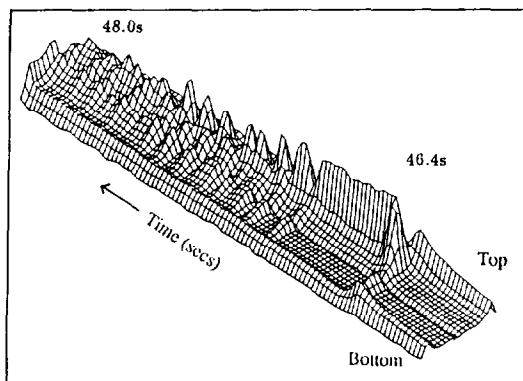


fig.3 Radiation profile along inner wall of JET

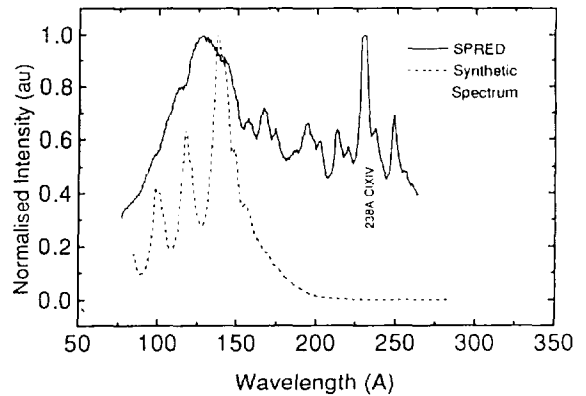


fig.4 VUV spectral feature with synthesised spectrum

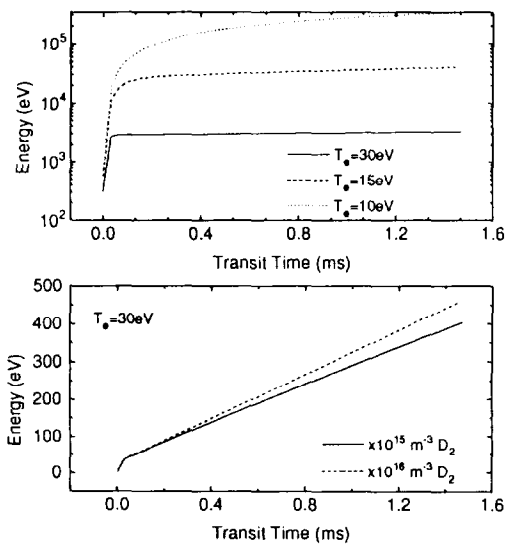


fig.5 Transient energy for (top) neutral carbon entering marfe region and (bottom) carbon streaming through marfe

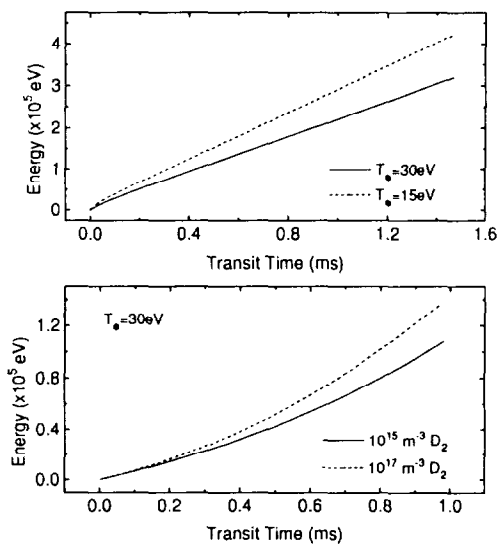


fig.6 Transient energy for (top) neutral nickel entering marfe region and (bottom) nickel streaming through marfe